Eliseevite, Na$_{1.5}$Li[Ti$_2$Si$_4$O$_{12.5}$(OH)$_{1.5}$]·2H$_2$O, a new microporous titanosilicate from the Lovozero alkaline massif (Kola Peninsula, Russia)

VICTOR N. YAKOVENCHUK,[1,2] GREGORY YU. IVANYUK,[1,2] SERGEY V. KRIVOVICHEV,[1,3,*]
YAKOV A. PAKHOMOVSKY,[1,2] EKATERINA A. SELIVANOVA,[2] JULIA A. KORCHAK,[2]
YURI P. MEN'SHIKOV,[2] SVETLANA V. DROGOBUZHSKAYA,[4] AND OLEG A. ZALKIND[4]

[1]Nanomaterials Research Center, Kola Science Center, Russian Academy of Sciences, 14 Fersman Street, Apatity 184200, Murmansk Region, Russia
[2]Geological Institute, Kola Science Center, Russian Academy of Sciences, 14 Fersman Street, Apatity 184200, Murmansk Region, Russia
[3]Department of Crystallography, Street Petersburg State University, 7–9 University Emb., Street Petersburg 199034, Russia
[4]Institute of Chemistry and Technology of Rare Elements and Mineral Recourses, Kola Science Center, Russian Academy of Sciences, 14 Fersman Street, Apatity 184209, Russia

ABSTRACT

Eliseevite, Na$_{1.5}$Li[Ti$_2$Si$_4$O$_{12.5}$(OH)$_{1.5}$]·2H$_2$O, is a new microporous titanosilicate of the lintisite-kukisvumite family [monoclinic, $C2/c$, $a = 27.48(1)$, $b = 8.669(4)$, $c = 5.246(2)$ Å, $\beta = 90.782(8)°$, $V = 1249.7(9)$ Å^3, $Z = 4$]. The mineral is found in two different peralkaline veins in an ijolite–foyaite–malignite differentiated complex of the Lovozero alkaline massif, Kola Peninsula, Russia. At Mt. Alluaiv, eliseevite occurs in an aegirine-eudialyte-sodalite-microcline vein as long-prismatic to fibrous crystals (up to 2 mm long) growing in voids of natrolitized sodalite in close association with albite, analcime, catapleiite, chabazite-Ca, gmelinite-K, manganoneptunite, microcline, murmanite, and an ussingite. At Mt. Punkaruaiv, it is found within a ussingite-aegirine-microcline vein as long-prismatic crystals (up to 0.8 mm long) in close association with chabazite-Ca, chkalovite, eudialyte, manganoneptunite, punkaruaivite, rhabdophane-(Ce), sodalite, sphalerite, and steenstrupine-(Ce). It is a late-stage, hydrothermal mineral formed as a result of alteration of murmanite. The mineral is transparent, pale creamy to colorless, with a vitreous luster and a white streak. Cleavage is perfect along {100}, fracture is splintery. Mohs hardness is about 5. In transmitted light, the mineral is colorless, biaxial (–): $\alpha = 1.665(2)$, $\beta = 1.712(2)$, $\gamma = 1.762(5)$ (for $\lambda = 589$ nm); $Y = b$, $Z\wedge a = 8$–12°. Dispersion is medium, $r < v$. $D_{calc} = 2.706$ g/cm^3, $D_{meas} = 2.68(4)$ g/cm^3. The mean chemical composition (n = 7) determined by the Penfield method (water), ICP-MS (Li), and electron microprobe (other elements) is (wt%): H$_2$O 10.50, Li$_2$O 2.85, Na$_2$O 9.15, K$_2$O 0.08, CaO 0.05, Fe$_2$O$_3$ 0.21, Al$_2$O$_3$ 0.08, SiO$_2$ 46.87, TiO$_2$ 29.40, Nb$_2$O$_5$ 0.72, total 99.91. The empirical formula calculated on the basis of Si = 4 apfu is: (Na$_{1.51}$K$_{0.01}$Ca$_{0.01}$)$_{\Sigma1.53}$Li$_{0.98}$[(Ti$_{1.89}$Nb$_{0.03}$Fe$^{3+}_{0.01}$Al$_{0.01}$)$_{\Sigma1.94}$Si$_4$O$_{12.26}$(OH)$_{1.74}$]·2.12H$_2$O. The simplified formula taking into account the results of a single-crystal study is Na$_{1.5}$Li{Ti$_2$O$_2$[Si$_4$O$_{10.5}$(OH)$_{1.5}$]}·2H$_2$O. The six strongest reflections in the X-ray powder-diffraction pattern [d in Å, (I), (hkl)] are: 13.76(100) (200), 6.296(60)(310), 3.577(80)(710), 3.005(70)(421), 2.881(70)(910), 2.710(50)(62$\overline{1}$). The mineral is named in honor of Nikolai Aleksandrovich Eliseev (1897–1966), a remarkable Russian geologist and petrologist, Professor at Leningrad State University, for his contributions to the geology and petrology of metamorphic and alkaline complexes.

Keywords: Eliseevite, new mineral, microporous titanosilicate, peralkaline hydrothermal formation, Lovozero massif, Kola Peninsula, Russia

INTRODUCTION

The ability of framework titanosilicates to extraframework-cation exchange and leaching often results in formation of new mineral species as a result of solid-state transformation of primary minerals (Khomyakov 1995, 2008). The most typical examples of such transformations are: kazakovite Na$_6$Mn^{2+}[TiSi$_6$O$_{18}$] → tisinalite Na$_3$Mn^{2+}Ti[Si$_6$O$_{15}$(OH)$_3$] (Khomyakov et al. 1978); vinogradovite Na$_5$[Ti$_4$(Si$_7$Al)O$_{26}$]·3H$_2$O → paravinogradovite Na[Ti$_4$(Si$_7$Al)(OH)$_4$O$_{22}$]·H$_2$O (Khomyakov et al. 2003); ivanyukite-Na-T Na$_2$K[Ti$_4$(OH)O$_3$(SiO$_4$)$_3$]·7H$_2$O → ivanyukite-Na-C NaK[Ti$_4$(OH)$_2$O$_2$(SiO$_4$)$_3$]·6H$_2$O → ivanyukite-K K[Ti$_4$(OH)$_3$O(SiO$_4$)$_3$]·9H$_2$O (Yakovenchuk et al. 2009). Cation-exchange properties of these phases are of interest from both mineral micro-evolution and technological points of view, because they may result in initiation of material research related to their applications in various areas of technology (Krivovichev 2008).

Yakovenchuk et al. (2010) demonstrated that lintisite, Na$_3$Li[Ti$_2$Si$_4$O$_{14}$]·2H$_2$O, transforms into punkaruaivite, Li[Ti$_2$Si$_4$O$_{11}$(OH)$_3$]·H$_2$O, due to the removal of Na$^+$ cations balanced by the Na$^+$ + O^{2-} ↔ □ + (OH)$^-$ substitution mechanism. Here we report the discovery of an intermediate product of this

transformation, which coexists with punkaruaivite without any reaction relation. Despite its intermediate character, it has its own chemical and structural stability field, which permitted us to consider it as a new mineral that was named eliseevite. The mineral name is in honor of Nikolai Aleksandrovich Eliseev (1897–1966), a remarkable Russian geologist and petrologist, Professor at Leningrad State University, in recognition of his contributions to the geology and petrology of metamorphic and alkaline complexes (Eliseev 1946, 1963; Eliseev and Nefedov 1940; Eliseev and Fedorov 1953).

The new mineral and its name were approved by the Commission on New Minerals, Classification and Nomenclature of the International Mineralogical Association (IMA 2010-031). The holotype material is deposited in the collections of the Mineralogical Museum of St. Petersburg State University (Russia) and of the Geological and Mineralogical Museum of the Geological Institute of the Kola Science Centre of the Russian Academy of Sciences (Apatity, Russia, catalog no. 6516).

Occurrence

The Lovozero alkaline massif is one of the largest (about 650 km^2) subvolcanic alkaline complexes in the world. It consists of numerous series of malignite-foyaite-foidolite layers consecutively intruded into Archean orthogneisses and Devonian volcanogenic-sedimentary rocks 360 million years ago (Kogarko et al. 1983). All of these rocks, especially malignites, usually have a characteristic trachitic texture (so-called "lujavrites"). The lower part of the layered complex (about 800 m thick) contains about 30 layers of loparite-rich ijolites and malignites, and the upper part (about 200 m thick) is enriched in eudialyte. The layered complex contains numerous conformal xenoliths of Devonian volcanic-sedimentary rocks (olivine basalts, basaltic tuffs, sandstones, and quartzites) and conformal lenses of poikilitic nepheline and sodalite-nepheline syenites, accompanied by numerous, usually also conformal pegmatite and hydrothermal veins and lenses.

Eliseevite was found in two hydrothermally altered ussingite pegmatites within the layered complex of malignites, foyaites, and foidolites with lenses of poikilitic nepheline syenites. At Mt. Alluaiv (type locality no. 1), it occurs within an aegirine-eudialyte-sodalite-microcline vein with nepheline, ussingite, murmanite, and magnesioarfvedsonite cropping out in the "Severny" loparite quarry (Yakovenchuk et al. 2010). The outer zone of the pegmatite (up to 80 cm thick) are composed of large blocks of microcline, nepheline, sodalite, and eudialyte penetrated by long-prismatic crystals of aegirine. Lamprophyllite, lorenzenite, and steenstrupine-(Ce) are present here in minor quantity.

The axial zone (up to 0.5 m thick) consists of sodalite, ussingite, eudialyte, albite, analcime, and natrolite (after ussingite, sodalite, and nepheline) with numerous inclusions of murmanite, magnesioarfvedsonite, nepheline, aegirine, lorenzenite, manganoneptunite, and chkalovite. Lomonosovite, β-lomonosovite, loparite-(Ce), epididymite, epistolite, ferronordite-(Ce), galena, keldyshite, lamprophyllite, löllingite, molybdenite, monazite-(Ce), pectolite, sphalerite, and steenstrupine-(Ce) occur as accessory minerals.

In areas of natrolitization, rock-forming minerals are altered (leached, hydrated, amorphised, replaced, etc.) giving rise to several secondary low-temperature minerals, including eliseevite. The mineral association consists of catapleiite, lovozerite, zircon, rhabdophane-(Ce), and terskite (after eudialyte); tugtupite and beryllite (after chkalovite); vinogradovite, goethite, and hemimorphite (after sphalerite); tvitusite-(Ce) (after belovite), and also hydroxycancrinite, chabazite-Ca and -K, phillipsite-Ca and -K, gmelinite-Ca and -K, and pyrite. Eliseevite is one of the latest minerals in this assemblage, forming colorless to pale creamy transparent long-prismatic crystals (up to 2 mm long) and sheaf-like aggregates (up to 5 mm long), sometimes covered by gmelinite and phillipsite, in voids within natrolitized ussingite and sodalite (Fig. 1).

At Mt. Punkaruaiv (locality no. 2), eliseevite was found in a ussingite-aegirine-microcline pegmatite lens (15 m diameter and up to 1.5 m thick) with concentric zoning (Yakovenchuk et al. 2010). The outer zone of the pegmatite (up to 30 cm thick) is composed of large tabular crystals of microcline, interstitial eudialyte, lorenzenite, aegirine, and murmanite. The intermediate zone (up to 30 cm thick) is formed by radiating aggregates of aegirine cemented by ussingite with inclusions of pseudomorphs of Mn hydroxides after crystals of pectolite–serandite and isometric crystals of manganoneptunite, belovite-(Ce), gerasimovskite, karnasurtite-(Ce), and catapleiite. Crystals of chabazite-Ca and heulandite-Ca incrust aegirine needles within large hollow spherulites.

The core (about 0.5 m thick) is composed of ussingite with relics of sodalite, segregations of murmanite and epistolite, eudialyte, chkalovite, manganoneptunite, and tainiolite, radiating aggregates of manganonordite-(Ce) and ferronordite-(Ce), grains and well-formed crystals of steenstrupine-(Ce), powder-like aggregates of rhabdophane-(Ce), grains of galena, sphalerite, and löllingite. Ussingite is partially replaced by natrolite, chkalovite is replaced by tugtupite and epididymite, galena is replaced by cerussite. Eliseevite occurs as radiated aggregates of colorless long-prismatic crystals (up to 0.5 mm long) that incrust cavities in ussingite together with punkaruaivite and gmelinite-Ca (Fig. 1).

PHYSICAL AND OPTICAL PROPERTIES

Eliseevite forms prismatic crystals elongated along the *c* axis and tabular on {100} with dominant {100}, {010}, and {001} forms. The *a:b:c* ratio calculated from the unit-cell parameters is 3.167:1:0.605 (calculated on the basis of X-ray powder-diffraction data). No twinning has been observed.
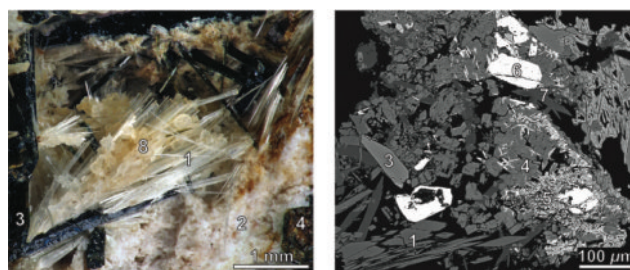

FIGURE 1. Long, prismatic eliseevite crystals (1) from the aegirine-eudialyte-sodalite-microcline vein in the foidolite-foyaite-malignite differentiated complex at Mt. Alluaiv, Lovozero Massif (type locality no. 1). 2 = natrolite, 3 = aegirine, 4 = eudialyte, 5 = zircon, 6 = belovite-(Ce), 7 = phillipsite-Ca, 8 = gmelinite-K. (Color online.)

Macroscopically, eliseevite is pale creamy to colorless with a vitreous luster. The mineral is translucent, with a white streak. Cleavage is perfect on {100}. Eliseevite is brittle and has a splintery fracture. The Mohs hardness is about 5. The density determined by the float and sink method in Clerici solution is 2.68(4) g/cm^3. This value is in a good agreement with the calculated density of 2.706 g/cm^3.

Eliseevite is biaxial negative; its refraction indices α = 1.665(2), β = 1.712(2), γ = 1.762(5) (for λ = 589 nm); $2V_{meas}$ = 85(5)°, $2V_{calc}$ = 89.3°. Optical orientation is $Y = b$, $Z\hat{}a$ = 8–12°. In transmitted light, the mineral is colorless, with a medium dispersion, $r < v$. A Gladstone-Dale calculation provides a compatibility index of 0.051, which is regarded as good (Mandarino 1981).

CHEMICAL COMPOSITION

The chemical composition of eliseevite has been studied by wavelength-dispersive spectrometry using a Cameca MS-46 electron microprobe (Geological Institute, Kola Science Centre of the Russian Academy of Sciences, Apatity) operating at 20 kV, 20–30 nA and 5 μm beam diameter. The following standards were used: lorenzenite (Na, Ti), pyrope (Al), diopside (Si, Ca), wadeite (K), hematite (Fe), and metallic niobium (Nb). Lithium content was determined using a Perkin Elmer ELAN 9000 DRC-e mass spectrometer equipped with an UP-266 MACRO laser probe (Institute of Chemistry and Technology of Rare Elements and Mineral Resources, Kola Science Center, Russian Academy of Sciences); NIST 612, punkaruaivite, and lintisite were used as standards. H$_2$O content was determined by the Penfield method for purified material from the type locality no. 1. Table 1 provides mean analytical results for three eliseevite crystals (where each analysis is the average of 6–10 point measurements). For comparison, we have given also composition of lintisite from the Sirenevaya vein at Mt. Alluaiv and punkaruaivite from the locality no. 2 at Mt. Punkaruaiv.

By analogy with the other minerals of the lintisite-kukisvumite family, the formula of eliseevite is calculated on the basis of Si = 4 as $(Na_{1.51}K_{0.01}Ca_{0.01})_{\Sigma 1.53}Li_{0.98}[(Ti_{1.89}Nb_{0.03}Fe^{3+}_{0.01}Al_{0.01})_{\Sigma 1.94}Si_4O_{12.29}(OH)_{1.71}]\cdot 2.14H_2O$. The simplified formula of eliseevite can be written as $Na_{1.5}Li[Ti_2Si_4O_{12.5}(OH)_{1.5}]\cdot 2H_2O$. The empirical formulas of lintisite and punkaruaivite are $Na_{2.95}Li_{0.98}[(Ti_{1.89}Nb_{0.05}Fe^{3+}_{0.02})_{\Sigma 1.96}Si_4O_{13.80}(OH)_{0.20}]\cdot 1.89H_2O$ and $(Na_{0.04}K_{0.01})_{\Sigma 0.05}Li_{1.01}[(Ti_{1.90}Nb_{0.04}Mn_{0.02}Fe^{3+}_{0.01})_{\Sigma 1.97}Si_4O_{10.96}(OH)_{3.04}]\cdot 1.21H_2O$, respectively. Thus, eliseevite is compositionally intermediate between lintisite and punkaruaivite, the transition being described by the Na$^+$ + O^{2-} $\leftrightarrow$ $\square$ + (OH)$^-$ substitution mechanism: $Na_3LiTi_2Si_4O_{14}\cdot 2H_2O$ → $Na_{1.5}LiTi_2Si_4O_{12.5}(OH)_{1.5}\cdot 2H_2O$ → $LiTi_2Si_4O_{11}(OH)_3\cdot H_2O$.

CRYSTAL STRUCTURE

Experimental methods

The crystal of eliseevite selected for data collection was mounted on a STOE IPDS II Image-Plate based X-ray diffractometer operated at 50 kV and 40 mA. More than a hemisphere of three-dimensional data was collected using monochromatic MoKα X-radiation, with frame widths of 2° in ω, and with a 180 s count for each frame. The unit-cell parameters (Table 2) were refined using least-squares techniques on the basis of 3422 reflections. The intensity data were integrated and corrected for Lorentz, polarization, and background effects using the STOE

TABLE 1. Chemical composition of eliseevite, lintisite, and punkaruaivite

	Eliseevite (locality no. 1)			Lintisite	Punkaruaivite
	Average	Range	Standard deviation	Khomyakov et al. (1990)	Yakovenchuk et al. (2010)
H$_2$O wt%	10.50			6.55	10.50
Li$_2$O	2.85			2.68	3.22
Na$_2$O	9.15	8.66–9.51	0.44	16.72	0.29
K$_2$O	0.08	0.00–0.23	0.13	0.03	0.14
CaO	0.05	0.00–0.14	0.08	0.00	0.01
MnO	0.21	0.18–0.26	0.04	0.05	0.31
FeO	0.08	0.00–0.24	0.14	0.28	0.21
Al$_2$O$_3$	46.87	46.81–46.94	0.14	0.00	0.05
SiO$_2$	29.40	28.71–29.98	0.64	44.03	51.35
TiO$_2$	0.72	0.40–0.95	0.28	27.68	32.50
Nb$_2$O$_5$	9.15	8.66–9.51	0.44	1.10	1.06
Total	99.93			99.12	99.64
Na apfu	1.51			2.95	0.04
K	0.01				0.01
Ca	0.01				
Li	0.98			0.98	1.01
Ti	1.89			1.89	1.90
Nb	0.03			0.05	0.04
Fe^{3+}	0.01			0.02	0.01
Mn					0.02
Al	0.01				
Si	4.00			4.00	4.00
H	5.99			3.98	5.47
O	16.14			15.89	15.20

program X-Area. The structure was solved by direct methods and refined to R_1 = 0.058. The SHELXL program package was used for all structural calculations (Sheldrick 1997). The final model included all atomic positional parameters, anisotropic-displacement parameters for all atoms and a refinable weighting scheme of the structure factors. The final atomic coordinates and anisotropic-displacement parameters are given in Table 3, and selected interatomic distances in Table 4. The list of observed and calculated structure factors can be provided by the authors upon request.

RESULTS

The structure of eliseevite is similar to those of vinogradovite (Rastsvetaeva and Andrianov 1984; Kalsbeek and Rønsbo 1992), lintisite (Merlino et al. 1990), kukisvumite (Merlino et al. 2000), and punkaruaivite (Yakovenchuk et al. 2010). It is based upon a 3D framework consisting of parallel chains of corner-

TABLE 2. Crystallographic data and refinement parameters for eliseevite

a (Å)	27.483(12)
b (Å)	8.669(4)
c (Å)	5.246(2)
β (°)	90.782(8)
V (Å^3)	1249.7(9)
Space group	C2/c
Z	4
D_{calc} (g/cm^3)	2.706
μ (mm^{-1})	1.81
F_{000}	1004
Crystal size (mm)	0.26 × 0.12 × 0.04
Radiation	MoKα
h_{min}, h_{max}	–34, 35
k_{min}, k_{max}	–11, 8
l_{min}, l_{max}	–6, 6
$2\theta_{min}, 2\theta_{max}$	2.46, 27.74
Total ref.	3358
Unique ref.	1343
Unique $|F_o| \geq 4\sigma_F$	959
R_1	0.058
wR_2	0.164
S	1.027
$\rho_{min}, \rho_{max}, e\cdot$Å^{-3}	–0.697, 1.202

sharing SiO$_4$ tetrahedra and chains of edge-sharing TiO$_6$ octahedra (Fig. 2a). From the structural point of view, eliseevite is an intermediate phase between lintisite, Na$_3$LiTi$_2$O$_2$[Si$_4$O$_{12}$] ·2H$_2$O, and punkaruaivite, LiTi$_2$(OH)$_2$[Si$_4$O$_{11}$(OH)]·H$_2$O. Transition from lintisite to punkaruaivite is associated with leaching of Na: eliseevite has only one Na site compared to two sites in lintisite. The Na1 site is 75% occupied, whereas the corresponding sites in punkaruaivite are empty.

The most unexpected feature of the structure of eliseevite is the location of Li in an octahedral instead of a tetrahedral site (as in lintisite and punkaruavite). The LiO$_6$ octahedron is strongly distorted with two short (1.81 Å) and four long (2.56–2.61 Å) Li$^+$-O bonds. Thus, Li occupies the site equivalent to the Na2 site in lintisite. Bond-valence analysis calculated using bond-valence parameters taken from Brown and Altermatt (1985) provides bond-valence sums of 4.21, 4.02, 4.09, 0.86, and 1.20 valence units (v.u.) for the Ti, Si1, Si2, Li, and Na sites, respec-

TABLE 3. Atomic coordinates, displacement parameters (Å^2), and site-occupancy factors (SOFs) for eliseevite

Atom	x	y	z	U_{iso}	SOF
Ti	0.1641(1)	0.4057(1)	0.1256(2)	0.0140(4)	1
Si1	0.2659(1)	0.5897(2)	0.2901(3)	0.0124(4)	1
Si2	0.0910(1)	0.0990(1)	0.0307(4)	0.0259(5)	1
Na	0.1655(1)	0.1972(4)	−0.3797(6)	0.0252(8)	0.75
O1	0.2070(1)	0.5773(4)	0.2890(8)	0.0148(9)	1
O2	0.2873(1)	0.7602(4)	0.2663(8)	0.0170(9)	1
O3	0.1049(2)	0.218(7)	0.3022(12)	0.048(2)	1
O4	0.1331(1)	0.4340(5)	0.4235(8)	0.0165(9)	1
O5	0.2873(1)	0.4920(5)	0.0490(7)	0.0148(9)	1
O6	0.1219(2)	0.2514(5)	−0.0083(8)	0.021(1)	1
OH7*	0.0329(2)	0.1310(7)	0.0142(11)	0.041(1)	1
H$_2$O8	−0.0376(4)	0.3854(12)	−0.049(3)	0.144(6)	1
Li	0	0.3675(14)	1/4	0.009(3)	1

Atom	U_{11}	U_{22}	U_{33}	U_{23}	U_{13}	U_{12}
Ti	0.0177(6)	0.0129(6)	0.0113(6)	0.0007(4)	−0.0001(4)	0.0002(4)
Si1	0.0172(9)	0.0114(8)	0.0087(8)	−0.0001(6)	−0.0003(6)	0.0001(6)
Si2	0.0234(10)	0.0197(10)	0.0347(12)	0.0006(8)	−0.0006(8)	−0.0012(7)
Na	0.034(2)	0.0204(17)	0.0211(17)	−0.0032(14)	0.0062(15)	0.0038(15)
O1	0.020(2)	0.015(2)	0.0096(19)	0.0002(15)	−0.0004(16)	−0.0013(16)
O2	0.024(2)	0.014(2)	0.013(2)	−0.0011(17)	−0.0039(17)	−0.0029(17)
O3	0.036(3)	0.044(3)	0.065(4)	0.034(3)	−0.007(3)	0.001(3)
O4	0.019(2)	0.020(2)	0.010(2)	−0.0019(16)	0.0024(16)	−0.0022(17)
O5	0.016(2)	0.019(2)	0.0096(19)	−0.0035(17)	0.0005(15)	−0.0012(17)
O6	0.030(2)	0.019(2)	0.015(2)	−0.0012(17)	0.0008(18)	−0.0055(18)
OH7	0.028(3)	0.055(3)	0.041(3)	0.010(3)	0.000(3)	0.013(2)
H$_2$O8	0.106(7)	0.105(8)	0.222(15)	−0.045(8)	0.105(9)	−0.027(6)
Li	0.002(6)	0.007(6)	0.019(7)	0	0.005(5)	0

* The occupancy of this site is (OH)$_{0.75}$O$_{0.25}$.

TABLE 4. Selected bond lengths (Å) in the structure of eliseevite

Ti-O4	1.806(4)	Na-O6	2.348(5)
Ti-O6	1.898(4)	Na-O5	2.382(5)
Ti-O2	1.917(4)	Na-O1	2.425(5)
Ti-O4	1.938(4)	Na-O4	2.458(5)
Ti-O1	2.077(4)	Na-O2	2.483(5)
Ti-O1	2.142(4)	Na-O5	2.707(5)
<Ti-O>	1.963	Na-O3	2.708(7)
		Na-O3	2.792(5)
Si1-O2	1.597(4)	<Na-O>	2.538
Si1-O1	1.620(4)		
Si1-O5	1.634(4)	Li-H$_2$O8	1.87(2) 2x
Si1-O5	1.638(4)	Li-OH7	2.56(1) 2x
<Si1-O>	1.622	Li-H$_2$O8	2.61(1) 2x
		<Li-O>	2.35
Si2-O6	1.587(5)		
Si2-O3	1.614(6)		
Si2-OH7	1.622(5)		
Si2-O3	1.641(6)		
<Si2-O>	1.616		

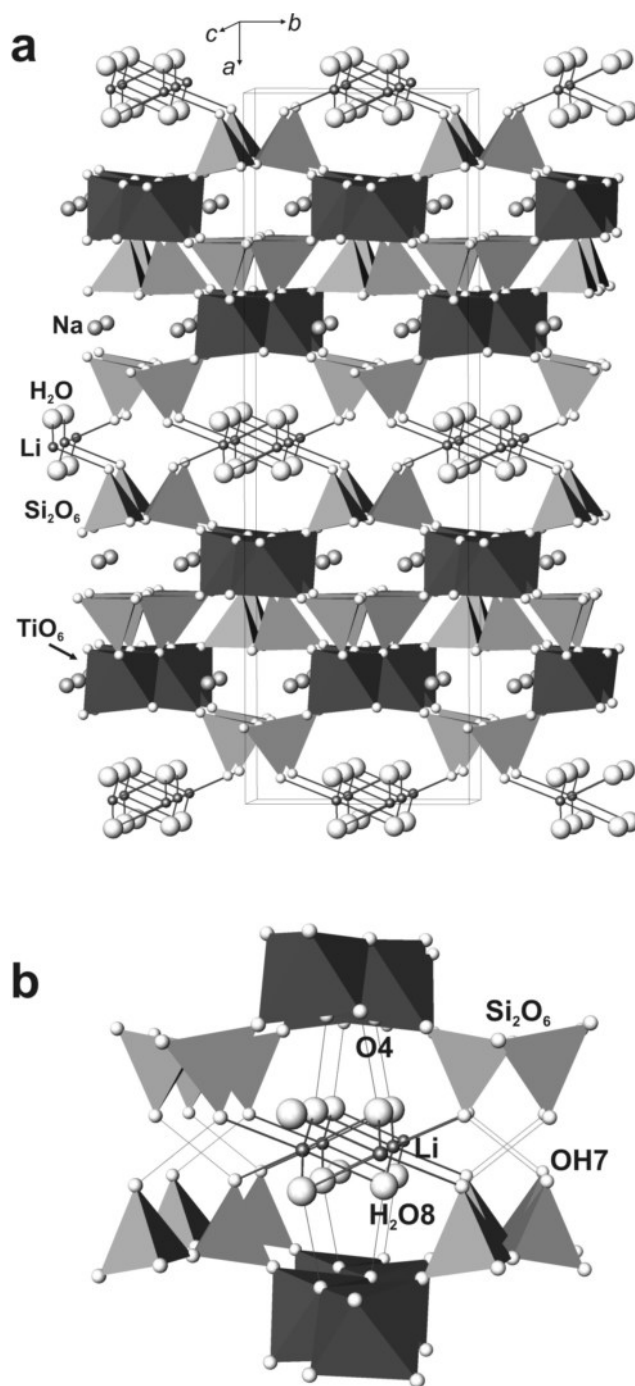**FIGURE 2.** The crystal structure of eliseevite (**a**) and the approximate scheme of hydrogen bonding inferred from the O···O distances (**b**) O···O contacts less than 3 Å are shown as thin lines).

tively. The bond-valence sum for the Na site is higher than the expected value (1); however, this site is only partially occupied and the bond-valence calculations are not really applicable to the disordered sites. The bond-valence sums for the O1, O3, O4, O5, and O6 sites are in the range from 1.91 to 2.24 v.u. The H$_2$O8 site receives 0.39 v.u. and can be unambigously assigned to the water molecule. The bond-valence sum incident upon the OH7 site is 1.06 v.u. that is characteristic for a hydroxyl

group. This site is a non-shared corner of the $Si2O_4$ tetrahedron and has a Si2-OH7 bond length of 1.622 Å. This bond length is typical for a silanol group (Nyfeler and Armbruster 1998). However, to achieve an electroneutrality of the whole structure, the OH7 site has been assigned the $(OH)_{0.75}O_{0.25}$ occupancy. The incorporation of O^{2-} anion into this site is most likely associated with distortion of the LiO_6 octahedron and probable formation of moderate hydrogen bonds to adjacent OH7 and H_2O8 sites located in the average structure at 2.905 and 2.951 Å, respectively.

Although we were unable to locate hydrogen positions, the hydrogen bonding scheme can be inferred from the analysis of the O···O distances. The H_2O8 site has the closest O···O contact at 2.748 Å to the O4 atom belonging to the TiO_6 octahedra (Fig. 2b). The OH7 site bonded to the Si atom of the silicate chain anion has the closest O···O contact at 2.904 Å to the OH7 site from the adjacent silicate chain. It seems possible that the protons, H^+, approximately occupies the same position as Li^+ in lintisite, Zn^{2+} in kukisvumite, and Mn^{2+} in manganokukisvumite, providing additional bonding between the adjacent titanosilicate two-dimensional blocks.

TABLE 5. X-ray powder diffraction data for eliseevite from locality no. 1*

I	d_{obs}, Å	d_{calc}, Å	*h k l*	*I*	d_{obs}, Å	d_{calc}, Å	*h k l*
100	13.76	13.734	2 0 0	1	2.461	2.462	4 0 $\overline{2}$
20	6.875	6.867	4 0 0			2.126	7 1 $\overline{2}$
60	6.296	6.296	3 1 0	40w	2.123	2.122	7 3 1
40	4.642	4.641	5 1 0			2.115	10 2 1
40	4.334	4.335	0 2 0	10	1.904	1.905	13 3 1
80	3.577	3.575	7 1 0	30	1.792	1.792	15 1 0
70	3.005	2.998	4 2 1	40	1.716	1.717	16 0 $\overline{0}$
70	2.881	2.879	9 1 0	10	1.662	1.661	2 4 $\overline{2}$
50	2.710	2.709	6 2 $\overline{1}$	30	1.623	1.623	0 2 3
10	2.583	2.584	2 0 $\overline{2}$	20	1.586	1.586	7 5 0
30	2.521	2.520	1 3 1				

* The standard deviation in d_{obs} is expected to be in the order of magnitude of the last reported figure.

Thus, the structural formula of eliseevite can be written as $Na_{1.5}Li\{Ti_2O_2[Si_4O_{10.5}(OH)_{1.5}]\}\cdot2H_2O$, which is in agreement with the results of chemical analysis.

X-ray powder diffraction

The powder X-ray diffraction pattern of eliseevite from type locality no. 1 was obtained by means of a URS-1 instrument operated at 40 kV and 30 mA with a Debye-Scherrer 114.7 mm in diameter camera and Fe$K\alpha$-radiation (Table 5). Unit-cell parameters determined from powder pattern are in agreement with those obtained from the single-crystal investigation: $a = 27.46(4)$ Å, $b = 8.67(1)$ Å, $c = 5.252(9)$ Å, $\beta = 90.6(4)°$, $V = 1251.1(8)$ Å^3.

Infrared spectroscopy

The infrared-absorption spectra of purified material of eliseevite, lintisite, and punkaruaivite were obtained using a Nicolet 6700 FTIR spectrometer and a press pellet of KBr at the Institute of Chemistry and Technology of Rare Elements and Mineral Resources (Kola Science Center, Russian Academy of Sciences). All three spectra are similar (Fig. 3), but the spectrum of eliseevite is much simpler and has much weaker bands of the Si-O stretching vibration at 930–1130 cm^{-1}. The strong bands at 400–500 cm^{-1} are probably caused by the Ti-O bending vibration. The O-H stretching vibrations of the H_2O molecules cause the intense broad band at 3430 cm^{-1} and the doublet at 2850–2920 cm^{-1}, of medium intensity. Medium strong band at 1630 cm^{-1} corresponds to the bending vibration of H_2O molecules.

DISCUSSION

A comparison of eliseevite, punkaruaivite, lintisite, kukisvumite, and manganokukisvumite (Table 6) permits us to consider these minerals as members of a separate mineral group, where the different mineral species are derived from the following three substitution schemes (Yakovenchuk et al. 2010):
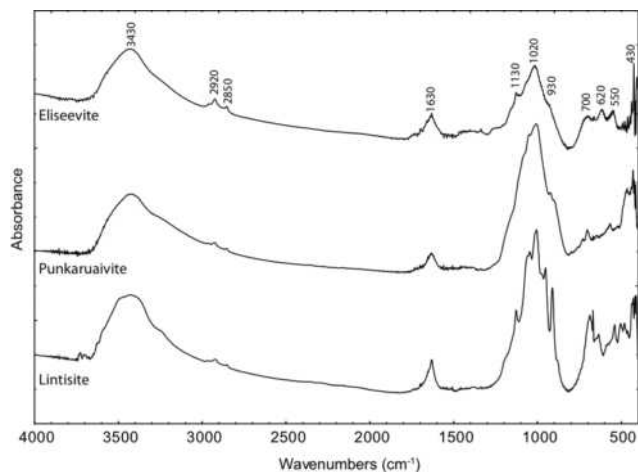
TABLE 6. Comparison of eliseevite, punkaruaivite, lintisite, kukisvumite, and mangano-kukisvumite

Mineral	Eliseevite $Na_{1.5}LiTi_2[Si_4O_{12.5}(OH)_{1.5}]\cdot2H_2O$	Lintisite* $Na_3LiTi_2[Si_4O_{14}]\cdot2H_2O$	Punkaruaivite† $LiTi_2[Si_4O_{11}(OH)_3]\cdot H_2O$	Kukisvumite‡ $Na_3Zn_{0.5}Ti_2[Si_4O_{14}]\cdot2H_2O$	Mangano-kukisvumite§ $Na_3Mn_{0.5}Ti_2[Si_4O_{14}]\cdot2H_2O$
Crystal system	monoclinic	monoclinic	monoclinic	orthorhombic	orthorhombic
Space group	*C2/c*	*C2/c*	*C2/c*	*Pccn*	*Pccn*
a (Å)	27.47	28.58	26.68	28.89	29.05
b (Å)	8.67	8.60	8.75	8.60	8.61
c (Å)	5.25	5.22	5.24	5.22	5.22
β (°)	90.6	91.0	91.2	90.0	90.0
Z	4	4	4	4	4
Strongest lines in powder pattern	13.76(100), 6.296 (60), 3.577 (80), 3.005 (70), 2.881 (70), 2.710 (50)	14.29 (100),6.39 (50), 4.77 (50), 3.69 (50), 2.744 (50), 2.709 (50)	13.3 (100), 6.23 (80), 4.38 (60), 3.50 (80), 3.01 (70), 2.81 (70)	14.49 (90), 6.42 (60), 4.815 (80), 4.302 (47), 3.722 (65), 3.009 (100)	14.47(100), 6.43 (20), 4.83 (10), 3.743 (10), 3.025 (40), 2.881 (20)
Density (g/cm^3)	2.68	2.77	2.60	2.90	2.86
Mohs hardness	5	5–6	4–5	5.5–6	5.5–6
Color	pale creamy to colorless	white	yellowish brown	white	colorless
Opt. character	biaxial (–)	biaxial (–)	biaxial (–)	biaxial (–)	biaxial (–)
α	1.665	1.672	1.658	1.676	1.657
β	1.712	1.739	1.696	1.746	1.744
γ	1.762	1.803	1.726	1.795	1.792
2*V* (°)	85	85	85	77	70
Orientation	$Y = b$, $Z\wedge a = 8$–12°	$Y = b$	$X = b$, $Z\wedge a = 12°$	$X = c$, $Z = a$	$X = a$, $Y = b$, $Z = c$
Dispersion	$r < v$, medium	$r < v$, strong	None observed	None observed	None observed
Pleochroism	None observed	None observed	$X =$ brownish-yellow, $Y =$ light brownish-yellow	None observed	None observed
Habit	Elongated (on *c*) tabular (on *a*) crystals	Elongated (on *c*) tabular (on *a*) crystals	Elongated (on *c*) tabular (on *a*) crystals	Elongated (on *c*) s tabular (on *a*) crystal	Elongated (on *c*) tabular (on *a*) crystals
Cleavage	{100} perfect	{100} perfect, {010} average	{100} perfect	{100} perfect	None observed

* Khomyakov et al. (1990).
† Yakovenchuk et al. (2010).
‡ Yakovenchuk et al. (1991).
|| Gault et al. (2004).

FIGURE 3. Infrared spectra of eliseevite, punkaruaivite, and lintisite.

(1) $2Li^+ \leftrightarrow Zn^{2+}$ (lintisite–kukisvumite series);
(2) $Zn^{2+} \leftrightarrow Mn^{2+}$ (kukisvumite–manganokukisvumite series);
(3) $Na^+ + O^{2-} \leftrightarrow \square + (OH)^-$ (lintisite–eliseevite–punkaruaivite series).

The crystal structures of all these minerals are based on pyroxene-like Si_2O_6 chains of corner-sharing SiO_4 tetrahedra and chains of edge-sharing TiO_6 octahedra. These vinogradovite-like titanosilicate blocks are linked into a framework by addition of ZnO_4, MnO_4, or LiO_4 tetrahedra (in kukisvumite, manganokukisvumite, lintisite, and punkaruaivite) or edge-sharing LiO_6 octahedra (in eliseevite).

According to the concept of transformation-induced minerals (Khomyakov 1995, 2008), both eliseevite and punkaruaivite are the results of the leaching of Na from lintisite by protonation reactions initiated by decreasing alkalinity of hydrothermal solutions. They can be considered as pseudomorphs forming by solid-state transformations of the primary lintisite. This kind of mineral behavior has recently been confirmed by our experimental studies, which demonstrated the possibility of single-crystal-to-single-crystal transformations during decationization reactions in lintisite; the results of these studies will be reported elsewhere.

ACKNOWLEDGMENTS

REFERENCES CITED

Brown, I.D. and Altermatt, D. (1985) Bond-valence parameters obtained from a systematic analysis of the Inorganic Crystal Structure Database. Acta Crystallographica, B41, 244–247.

Eliseev, N.A. (1946) Devonian effusive rocks of the Lovozero Tundra. Zapiski Vsesoyuznogo Mineralogicheskogo Obshchestva, 752, 113–134 (in Russian).
——— (1963) Metamorphism. Nedra, Moscow (in Russian).
Eliseev, N.A. and Fedorov, E.E. (1953) The Lovozero Massif and its Mineral Deposits. AN SSSR Press (in Russian).
Eliseev, N.A. and Nefedov, N.K. (1940) Loparite deposits of the Luyavrurt. The industrial potential of the Kola Peninsula, 1, 77–118 (in Russian).
Gault, R.A., Ercit, T.S., Grice, J.D., and van Velthuizen, J.V. (2004) Manganokukisvumite, a new mineral species from Mont Saint-Hilaire, Quebec. Canadian Mineralogist, 42, 781–785.
Kalsbeek, N. and Rønsbo, J.G. (1992) Refinement of the vinogradovite structure, positioning of Be and excess Na. Zeitschrift für Kristallographie, 200, 237–245.
Khomyakov, A.P. (1995) Mineralogy of Hyperagpaitic Alkaline Rocks. Clarendon Press, Oxford, U.K.
——— (2008) The largest source of minerals with unique structure and properties. In S.V. Krivovichev, Ed., Minerals as Advanced Materials I, p. 71–77. Springer, Berlin.
Khomyakov, A.P., Kaptsov, V.V., Shchepochkina, N.I., Rudnitskaya, E.S., and Krutetskaya, L.M. (1978) Phenomenon of ultra-quick hydrolysis of hyperalkaline titano- and zirconosilicates. Experimental testing. Doklady Akademii Nauk SSSR, 243, 1028–1031 (in Russian).
Khomyakov, A.P., Polezhaeva, L.I., Merlino, S., and Pasero, M. (1990) Lintisite, Na₃LiTiSi₄O₁₄·2H₂O—a new mineral. Zapiski Vsesoyuznogo Mineralogicheskogo Obshchestva, 119, 76–80.
Khomyakov, A.P., Kulikova, I.E., Sokolova, E., Hawthorne, F.C., and Kartashov, P.M. (2003) Paravinogradovite, (Na,□)₂[(Ti, Fe)₄(Si₂O₆)₂(Si₃AlO₁₀)(OH)₄]·H₂O, a new mineral species from the Khibina alkaline massif, Kola Peninsula, Russia: description and crystal structure. Canadian Mineralogist, 41, 989–1002.
Kogarko, L.N., Kramm, U., and Grauert, B. (1983) New data on age and genesis of alkaline rocks of Lovozero massif (rubidium and strontium isotopy). Doklady Akademii Nauk SSSR, 268, 970–972 (in Russian).
Krivovichev, S.V. (Ed.) (2008) Minerals as Advanced Materials I. Springer, Berlin.
Mandarino, J.A. (1981) The Gladstone-Dale relationship. IV. The compatibility concept and its application. Canadian Mineralogist, 19, 441–450.
Merlino, S., Pasero, M., and Khomyakov, A.P. (1990) The crystal structure of lintisite, Na₃LiTi₂(Si₂O₆)₂O₂·2H₂O, a new titanosilicate from Lovozero (USSR). Zeitschrift für Kristallographie, 193, 137–148.
Merlino, S., Pasero, M., and Ferro, O. (2000) The crystal structure of kukisvumite, Na₆ZnTi₄(Si₂O₆)₄O₄·4(H₂O). Zeitschrift für Kristallographie, 215, 352–356.
Nyfeler, D. and Armbruster, T. (1998) Silanol groups in minerals and inorganic compounds. American Mineralogist, 83, 119–125.
Rastsvetaeva, R.K. and Andrianov, V.I. (1984) Refined crystal structure of vinogradovite. Soviet Physics Crystallography, 29, 403–406.
Sheldrick, G.M. (1997) SHELXL97. Program for the Refinement of Crystals Structures. University of Göttingen, Germany.
Yakovenchuk, V.N., Pakhomovskii, Y.A., and Bogdanova, A.N. (1991) Kukisvumite—a new mineral from the alkaline pegmatites of the Khibiny massif (Kola Peninsula). Mineralogicheskiy Zhurnal, 13, 63–67 (in Russian).
Yakovenchuk, V.N., Nikolaev, A.P., Selivanova, E.A., Pakhomovsky, Ya.A., Korchak, J.A., Spiridonova, D.V., Zalkind, O.A., and Krivovichev, S.V. (2009) Ivanyukite-Na-T, ivanyukite-Na-C, ivanyukite-K, and ivanyukite-Cu: New microporous titanosilicates from the Khibiny massif (Kola Peninsula, Russia) and crystal structure of ivanyukite-Na-T. American Mineralogist, 94, 1450–1458.
Yakovenchuk, V.N., Ivanyuk, G.Yu., Pakhomovsky, Ya.A., Selivanova, E.A., Men'shikov, Yu.P., Korchak, J.A., Krivovichev, S.V., Spiridonova, D.V., and Zalkind, O.A. (2010) Punkaruaivite, LiTi₂[Si₄O₁₁(OH)](OH)₂·H₂O, a new mineral species from hydrothermal assemblages, Khibiny and Lovozero Alkaline Massifs, Kola Peninsula, Russia. Canadian Mineralogist, 48, 41–50.